nature genetics

Supplementary information

https://doi.org/10.1038/s41588-025-02269-0

Uncovering the multivariate genetic architecture of frailty with genomic structural equation modeling

In the format provided by the authors and unedited

Supplementary Note

Table of Contents

Supplementary Methods

Trait Selection and Multivariable Linkage Disequilibrium Score Regression

After selecting the initial 52 frailty deficits (**Main Text** and **Supplementary Table 1**), we conducted multivariable linkage disequilibrium score regression (LDSC) to perform a series of pre-determined quality control checks to decide which frailty deficits could be reliably included in our subsequent analyses.

We performed multivariable LDSC using the *GenomicSEM* R package and publicly available LD scores and weights from the 1000 Genomes Phase 3 European reference panel that excluded the major histocompatibility complex (MHC) owing to its complex patterns of LD(1, 2). LDSC was applied to estimate a genetic covariance matrix with SNP-based heritability (h^2_{SNP}) of each phenotype on the diagonal and the genetic covariance across each pairwise combination of traits on the off-diagonal. Multivariable LDSC also produces a sampling covariance matrix that includes the sampling variances (i.e., the squared standard errors) of the estimates on the diagonal and the sampling dependencies on the off diagonal that can arise due to participant sample overlap. This sampling covariance matrix is estimated directly from the GWAS data and is what allows genomic structural equation modelling (Genomic SEM) to produce appropriate estimates for traits with varying levels of precision (e.g., with different participant sample sizes) and varying and unknown levels of sample overlap. This was important for producing interpretable results within the current study, wherein our frailty deficits varied widely with respect to statistical power. Prior to running LDSC, each of the GWAS summary statistic datasets underwent a uniform formatting and quality control step. This included removing SNPs with a minor allele frequency (MAF) below 0.01 and an imputation score (INFO) below 0.9, restricting SNPs to HapMap 3 SNPs, and aligning all GWAS effects to the same reference allele(3). For all genome-wide analyses, we used a false discovery rate (FDR) corrected *q*-value threshold of <0.05 to account for multiple testing.

Traits were removed from further analyses if they had a h^2_{SNP} Z-statistic ≤4 as these can yield unstable estimates of genetic overlap(4). We converted heritability estimates to the liability scale for binary traits using population prevalence values based on recent epidemiological estimates for European ancestral populations (**Supplementary Table 1**)(5-14). The sum of effective sample sizes across the cohorts that had contributed to that GWAS was used to adjust for cohort-specific ascertainment(15).

We also calculated the pairwise genetic correlation (r_g) between all 52 frailty deficits using multivariable LDSC to further assess which frailty deficits should be included in the final model. The results from the genetic correlation analysis (**Supplementary Figure 1** and **Supplementary Table 2**) were used to perform additional quality control, where deficits were brought forward for subsequent analysis providing they met the following criteria: (*i*) in instances where two traits were highly multicollinear (r_g ≥0.9), we removed the trait in the pair that had the lowest mean genetic correlation (r_g) with the other traits; *(ii*) we removed traits that had low mean genetic correlations with the other traits (mean r_g ≤0.10) as these traits are not empirically indicated to be part of the broader multivariate genetic architecture of frailty; (*iii*) for phenotypically similar traits (e.g., number of cigarettes smoked per day vs smoking initiation), we retained the deficit with the highest mean r_g with all other deficits.

In total, we excluded 22 frailty deficits, which did not meet the described criteria for inclusion. Number of self-reported cancers was removed due to having a very low SNP-based heritability (h^2_{SNP} = 0.01, SE = 0.001) since this meant that it did not have enough genetic signal to be meaningfully modelled using Genomic SEM. Five frailty deficits (broad depression, anxiety, falls risk, systolic blood pressure and number of treatments/medications taken) were removed because they displayed high multicollinearity (r_g ≥ 0.9) with another included deficit (major depressive disorder (for both broad depression and anxiety), number of falls per year, mean arterial pressure and number of self-reported illnesses, respectively). Such high genetic correlation estimates demonstrated that there was near complete genetic overlap between these pairs of frailty deficits, so including both into the model did not make sense because they

were essentially representing the same phenotype twice, which would have created a separate latent factor in the model that was not representing general frailty pathways.

A further five frailty deficits (reaction time, heel bone mineral density, low-density lipoprotein (LDL) cholesterol, constipation, low frequency of friends and family visits) were removed because they had low mean genetic correlations with the included deficits (mean $r_g \leq 0.10$), which meant that they were nearly completely genetically distinct from the other frailty deficits and therefore would not have fit well into a latent factor model of shared frailty pathways. It should be noted that this does not negate the importance of these factors in the pathogenesis and clinical manifestations of frailty, but simply indicates that there are certain frailty deficits that are more biologically distinct and so may drive independent pathways to frailty compared to other highly pleiotropic deficits where their underlying biology converges to drive frailty onset. Since the remit of this study was to model the patterns of shared genetic pathways between frailty deficits, we only included those that had meaningful overlap with other deficits.

Finally, eleven frailty deficits (excessive daytime sleepiness, fed-up feelings, smoking initiation, duration of walking per day, disability allowance, dentures, forced vital capacity, peak expiratory flow, financial satisfaction, friendship satisfaction and family relationship satisfaction) were removed because they were phenotypically similar to another deficit but had a lower mean genetic correlation with the other deficits. We intentionally began with a higher number of potential frailty deficit phenotypes because this is the first application of Genomic SEM being used to define frailty and so we wanted to ensure that we selected the most powerful GWAS phenotypes into our model that had both a meaningful level of genetic signal and correlation between other deficits. Therefore, the final 30 deficits should be regarded as each representing a distinct aspect of the frailty state at the genetic level, which provided the strongest foundation for modelling their shared influences on frailty pathogenesis.

This resulted in a final list of 30 traits that were brought forward for all subsequent analyses (**Supplementary Table 1**).

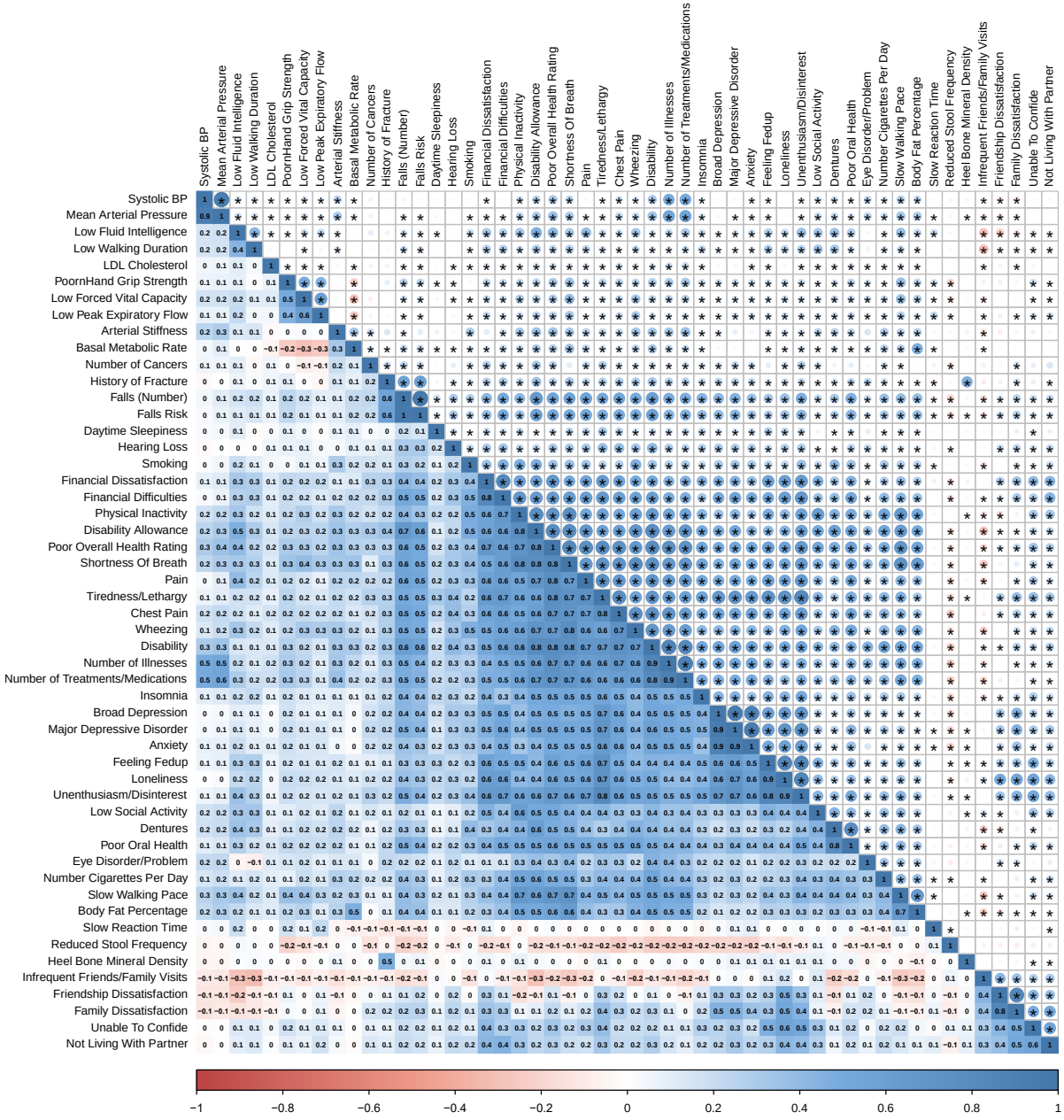

Supplementary Figure 1: A heatmap of the pairwise genetic correlations between the 52 frailty deficits estimated using multivariable linkage disequilibrium score regression. Deficits are ordered using hierarchal clustering to help visualize the underlying patterns of correlations between the frailty deficits. All deficits are coded to represent the frailty-inducing phenotype. Blue shading represents a positive genetic correlation whereas red shading represents a negative genetic correlation. Genetic correlation coefficients are shown on the bottom triangle of the matrix and the upper triangle is marked with an asterisk if the genetic correlation was statistically significant after multiple testing correction (i.e. a False Discovery Rate (FDR) corrected two-sided q-value < 0.05). BP = blood pressure; LDL = low-density lipoprotein.

Multivariate GWAS of the Latent Frailty Model

Data Standardization. In order to measure the individual SNP associations with the latent factors in our frailty model, we initially used the *sumstats* function in the *GenomicSEM* R package to create a standardized data file that converted the SNP effect estimates from each univariate GWAS into covariances between each individual SNP and the overall phenotypic variance of each deficit and standardized the SNP effects relative to the phenotypic variance

of the trait(3). This allowed these SNP effects to be added to the genetic covariance matrix as they were then on the same scale as the LDSC estimates. All phenotypes were based on genome build 37 (GRCh37/hg19) or were converted from build 38 using the *MungeSumstats* R package(16). We removed any SNPs that had a MAF <0.01 or an INFO score <0.6. We used the 1000 Genomes Phase 3 European ancestry dataset as our reference genome and aligned SNPs to have the same effect (A1) and non-effect (A2) allele across phenotypes. SNPs were removed if either the effect or non-effect allele did not match the reference genome. As *sumstats* performs listwise deletion across the included traits only SNPs that had been measured in all the contributing univariate GWASs were included, resulting in a final harmonized dataset of 5,849,452 SNPs for multivariate GWAS analysis. The standardized GWAS data and LDSC results were used as input for calculating multivariate GWAS of the frailty latent factors using the *userGWAS* function in the *GenomicSEM* R package.

Gene Mapping and Pathway Analysis

As outlined in the main text, we used five gene mapping methods (i.e. positional mapping, expression quantitative trait loci (eQTL) mapping, chromatin interaction mapping, MAGMA and multi-SNP summary data-based Mendelian randomization (SMR-multi)) to identify potentially causal genes for each of the identified risk loci in our multivariate GWAS, which we then used to prioritize genes to be included in our subsequent pathway analysis.

Positional, eQTL and chromatin interaction mapping. We performed positional, eQTL and chromatin interaction mapping with FUMA(17). This involved positionally mapping candidate SNPs to their closest protein-coding gene (within a 10kb window upstream or downstream of the SNP location). We conducted eQTL mapping to ascertain whether the candidate SNPs in our latent factor GWAS loci are known regulators of gene expression, which we defined as any eQTL-gene interaction displaying an FDR-corrected *q*-value ≤ 0.05 to account for multiple testing(17). Since frailty represents a multi-system clinical state, we integrated publicly available eQTL data for multiple body tissues and cell types with our GWAS results to provide a broad overview of the potential impacts that the risk loci for frailty have on gene expression. This included integration of eQTL data from 15 repositories including the Blood eQTL Browser(18), BIOS QTL browser(19), BRAINEAC(20), MuTHER(21), xQTLServer(22), CommonMind Consortium(23), eQTLGen(24), PsychENCODE(25), DICE(26), scRNA eQTLs(27), eQTL Catalogue(28-44), GTEx v8(45), EyeGEx(46), InsPIRE(47) and TIGER(48). Finally, we conducted chromatin interaction mapping, which involved annotating candidate SNPs that displayed a significant 3D chromatin interaction (FDR-corrected q-value ≤ $1x10^{-6}$) with a known gene region based on pre-processed chromatin loop data and enhancer-promoter link data for multiple body tissues from 4 publicly available databases(25, 49-51). We restricted successful mappings of SNPs to those where the candidate SNP overlapped with the enhancer region within one of the selected epigenomes and the promoter region of the mapped gene overlapped with the promoter region of the associated epigenome. Enhancer and promotor information was obtained for 111 epigenomes from the Roadmap Epigenomics Project(52).

Summary Data-Based Mendelian Randomization. Next, we applied multi-SNP summary data-based Mendelian randomization (SMR-multi) to our GWAS results for each latent factor to identify whether there was any evidence that the identified genomic risk loci had an influence on gene expression (eQTLs), splicing ratios (sQTLs) or methylation status (mQTLs). Mendelian randomization (MR) relies on 3 core assumptions being met(53). First, the *independence assumption* states that there should be no association between the IV and confounders of the exposure-outcome relationship. Since the allocation of alleles is randomly assigned at conception, the use of genetic variants as the IV minimizes the risk of the independence assumption being violated because unmeasured confounders should then be randomized across the population in a fashion that is akin to a randomized controlled trial. Second, the *relevance assumption* states that the IV is associated with the exposure of interest. To satisfy the relevance assumption, SNPs that had a strong association (P_{QTL} < $5x10^{-8}$) with the QTL region (i.e. expression, splicing or methylation) in each QTL dataset were selected as instrumental variables for SMR-multi analysis(54). Variants in high LD with the lead SNP in a region (R^2 > 0.9) were removed using the 1000 Genomes phase 3 European data as a reference. We then applied FDR correction across all the results (i.e. all tests conducted across all latent factors and all QTL datasets) and filtered our results to only include SMR associations with a q-value$_{SMR}$ < 0.05. Finally, the *exclusion restriction* assumption states that there should be no direct pathways between the IV and the outcome (i.e., the relationship between the IV and outcome operates strictly via the exposure variable). A key difference

between SMR and traditional MR is that the exclusion restriction assumption need not hold for SMR. This is because SMR seeks to identify both pleiotropic (i.e. both the QTL and the frailty outcome are affected by the same causal variant) and causal pathways (i.e. the effect of the genetic variant on the frailty outcome is mediated via its effect on a QTL) between the exposure and outcome, rather than focusing solely on causal pathways(55). With that said, confounding due to linkage (i.e., association between exposure and outcome due to independent causal SNPs being in LD with one another) can bias SMR as it may inappropriately infer shared biology(53). Therefore, to distinguish pleiotropy from linkage we used the heterogeneity in dependent instruments (HEIDI) test using the default parameters to measure whether the association patterns within an instrumental variable were homogenous between the QTL exposure and the frailty outcome, and we rejected any associations that demonstrated significant heterogeneity ($P_{HEIDI} < 0.01$)(54).

We used pre-processed data curated by the original method developers to construct the instrumental variables (IVs) for our functional exposures, which included eQTL data from BrainMeta v2(56), CAGE(57), GTEx v8(45), GEUVADIS(35) and PsychENCODE (corrected for 100 hidden covariate factors)(58); sQTL data from BrainMeta v2(56) and GTEx v8(45); and mQTL data from Brain-mMeta(59) and McRae et al(54, 60) (**Table 1**). All data was based on genome build 37 (GRCh37/hg19) and we aligned the GWAS data and QTL data to the same effect and non-effect alleles using the 1000 Genomes phase 3 European data as our reference. We converted the MAF column in the GWAS summary statistics into the effect allele frequency (EAF) by integrating data on the major allele for each SNP from dbSNP v155. Any SNPs that had a discrepant allele frequency >0.20 between the GWAS and QTL data or that were located within the extended MHC region (chr6:28477797-chr6:33448354) were omitted from the analysis(54).

Table 1: An overview of the datasets used for Summary Data-Based Mendelian randomization.

Name of Dataset	Type of data	Tissue/cell type	Sample size and details
BrainMeta (version 2)	eQTL & sQTL	Brain cortex	2,443 unrelated individuals of European ancestry from 7 cohorts
Consortium for the Architecture of Gene Expression (CAGE)	eQTL	Peripheral blood	2,765 individuals from 5 cohorts
Genotype-Tissue Expression (GTEx) Consortium version 8	eQTL & sQTL	49 tissues/cell types	15,201 samples from 838 donors (all tissues/cell lines had to have samples from >70 individuals to be included)
Genetic European Variation in Disease (Geuvadis) Consortium	eQTL	Lymphoblastoid cell lines	373 individuals of European ancestry from the 1000 Genomes project
PsychENCODE	eQTL	Prefrontal Cortex	Post-mortem samples from 1,387 individuals from 8 cohorts
McRae Group	mQTL	Peripheral blood	1,980 individuals of European ancestry from 2 cohorts (Lothian Birth Cohorts and the Brisbane Systems Genetics Study)
Brain-mMeta	mQTL	Brain cortex	A meta-analysis of dorsolateral prefrontal cortex samples from 468 older adults in ROSMAP, 166 fetal brain (prefrontal cortex, striatum and cerebellum) samples from Hannon et al and 526 prefrontal cortex samples from Jaffe et al. This produced an estimated effective N of 1,160 individuals.

Pathway Analysis. As outlined in the main text, we used the results from the 5 gene mapping methods to guide gene prioritization. Any genes that were mapped to a latent factor by 3 or more methods were taken forward for subsequent pathway analysis. We performed pathway enrichment analysis using METASCAPE(61). Since the General Factor was orthogonal to the six latent residual group factors in our model (i.e. Factors 1-6), we conducted a single standalone pathway enrichment analysis for the General Factor prioritized genes because, by definition, the genetics underpinning this latent factor are uncorrelated with the genetics driving the other latent factors. We then performed a separate combined

enrichment analysis of the prioritized genes for Factors 1-6 as this enabled us to explore what biology might be driving the inter-factor correlations that we saw in our model. The prioritized genes were assigned to any curated gene set they belonged to using data from Gene Ontology (GO) Biological Processes (1495 gene sets)(62), the Human Molecular Signatures Database (MSigDB) Canonical Pathways (17 gene sets)(63), Reactome (262 gene sets)(64), Kyoto Encyclopedia of Genes and Genomes (KEGG) Pathways (113 gene sets)(65), WikiPathways (89 gene sets)(66) and DisGeNET (2050 gene sets)(67). The default hypergeometric test method was used to calculate enrichment for each gene set that included ≥ 1 of the prioritized genes and FDR correction was applied to correct for multiple testing(61). However, many of the gene ontology terms overlap, which leads to high levels of redundancy in the results, so we performed the recommended clustering analysis that combined related gene sets into groups by calculating the pairwise similarities between all enriched terms based on their Kappa-test score and hierarchally ordered them within a similarities matrix (Kappa similarities > 0.3 were combined)(61). In the case of the multi-gene-list enrichment test for the analysis of Factors 1-6, this enrichment test was initially performed on each of the latent factor gene lists separately, followed by an additional test that combined the gene lists across all six latent factors to determine whether there were enriched gene ontology terms that were shared across the latent factors. This was appropriate since our initial results demonstrated that there was significant correlation between certain latent factors in our model.

Cohort Samples Used for the Main Polygenic Risk Score Analyses

Lothian Birth Cohort 1936 (LBC1936). LBC1936 is a longitudinal study of community dwelling older adults living in and around Edinburgh, Scotland (United Kingdom)(68). Individuals joined the study when they initially took part in the Scottish Mental Survey in 1947 and have thus far taken part in 5 waves of testing. The main analyses, when examining frailty outcomes, were performed on wave 1 (mean age = 69.60; SD = 0.83; *N* = 1005 (509 males, 496 females)). Ethics for LBC1936 was approved by the Multi-Centre Research Ethics Committee for Scotland (Wave 1: MREC/01/0/56), the Lothian Research Ethics Committee (Wave 1: LREC/2003/2/29), and the Scotland A Research Ethics Committee (Waves 2, 3, 4 and 5: 07/MRE00/58) and all methods were performed in accordance with the relevant guidelines and regulations. Informed Written Consent was obtained from participants at each of the waves.

The genotypes, which were collected via blood samples from the participants at Wave 1 were processed using stringent quality control measures(69). Genotyping was conducted using the Illumina Human610-Quadv1 chip, with 542,050 SNPs passing quality control. Out of 1,091 individuals in the LBC1936 cohort, genomic DNA from 1,071 individuals was successfully isolated using standard procedures at the Wellcome Trust Clinical Research Facility (WTCRF) Genetics Core. Twenty-nine samples did not meet quality control standards before genotyping. The remaining 1,042 blood-extracted samples were genotyped at the WTCRF Genetics Core with the Illumina Human610-Quadv1 chip, and SNPs were imputed to the 1000 Genomes reference panel (phase 1, version 3). After undergoing the described quality control procedures, samples from 1,005 individuals were retained for analysis.

English Longitudinal Study of Aging (ELSA). ELSA is a longitudinal panel study of community dwelling adults aged 50 years and over residing in England (United Kingdom)(70). For the main ELSA analysis, a sample of 7181 adults (3325 males and 3856 females) was analyzed, with a mean age of 68.45 (SD = 10.13; age range = 50-99 years). This represents individuals who have taken part in the study between 2002/3 to 2018/19. Previous work has shown that the year/wave that the participant entered the study does not affect the relationship between polygenic prediction scores and frailty outcomes(71). Ethical approval for ELSA was gained via the South Central – Berkshire Research Ethics Committee (21/SC/0030, 22nd March 2021) and all methods were performed in accordance with the relevant guidelines and regulations.

The ELSA genetics team approved a request for this study to utilize raw genotypes and provided linked genome-wide association study (GWAS) data to the phenotypic data curated at the Advanced Care Research Centre, University of Edinburgh(71). The genome-wide genotyping was conducted by

University College London (UCL) Genomics between 2013 and 2014. This process involved genotyping 7,597 ELSA participants of European ancestry using Illumina HumanOmni2.5 BeadChips (HumanOmni2.5-4v1, HumanOmni2.5-8v1.3), which assess approximately 2.5 million markers capturing genomic variation down to a minor allele frequency (MAF) of 2.5%. The genotyping was completed in two separate batches. After filtering for 5% missing data, allele frequencies were compared between the batches, showing a correlation of over 99% across several chromosomes. Following post-genotyping quality control, which included removing ancestral outliers (self-reported) and duplicates, the final genotyped dataset comprised 7,412 ELSA participants and 2,230,767 SNPs. Imputation was performed via the Michigan Imputation Server using SHAPEIT for pre-phasing and Minimac3 for imputation, with the Haplotype Reference Consortium (HRC.r1-1.GRCh37) as the reference panel, aligning all variants to genome build 37 (hg19).

Prospective Imaging Study of Aging (PISA). PISA is a longitudinal cohort of ~3800 Australian adults aged 40-80 years(72). Since this cohort includes twin pairs, we selected one of each pair at random to be included in our current analyses. When the Frailty Index (FI) was derived and linked with genotypic data, 3265 participants (1034 males and 2231 females) remained for the main analysis, with a mean age of 60.34 (SD = 6.98). The PISA study protocol was approved by the Human Research Ethics Committee (HREC) at QIMR Berghofer Medical Research Institute.

Participants are community dwelling and were recruited from a pool of participants who previously volunteered for research on risk factors for physical or psychiatric conditions and had genotypes already available. Genome-wide genotyping of participants was previously conducted using various genotyping arrays, including Illumina chips based on HapMap references (317 K, 370 K, 610 K, 660 K) and more recent Illumina arrays based on the 1KGP reference (Core + Exome, PsychArray, OmniExpress) as detailed in earlier studies(73, 74). All datasets have been combined following rigorous quality control procedures and imputed using the Haplotype Reference Consortium (HRC) Release 1 reference panel(75).

Cohort Samples Used for Age-Stratified Polygenic Risk Score Analyses

To understand the effect of the polygenic risk scores (PRS) of the frailty latent factors as individuals age, we performed additional age-stratified analyses in each of the external cohorts. For LBC1936 we used data from waves 3 and 5 to utilize all the longitudinally measured waves in which the relevant data was present. The mean age at Wave 3 was 76.30 (SD = 0.68; *N* = 649 (339 males, 310 females)) and was 82.06 at Wave 5 (SD = 0.53; *N* = 402 (196 males, 206 females)). We utilized these data for the univariate PRS analyses to predict the efficacy of the latent frailty factors in predicting Frailty Index (FI) and Fried Frailty Phenotype (FP) status in these waves of data, but we did not perform the age-stratified multivariate elastic net regression analyses with LBC1936 data owing to small sample sizes for waves 3 and 5.

To understand the effect of age on the prediction of FI status for individuals in ELSA and PISA, we additionally ran both the univariate regression PRS analyses and the multivariate elastic net regression PRS analyses on a subset of the main ELSA and PISA samples that were aged ≥ 65 years old (PISA: mean age = 68.55, SD = 2.82, *N* = 991 (372 males, 619 females); ELSA: mean age = 68.55, SD = 2.82, *N* = 4407 (2066 males, 2341 females)).

Frailty Outcomes Used for Polygenic Risk Score Prediction

Frailty Index (FI). This measure was created in each of the external cohorts (LBC1936, ELSA and PISA) and includes frailty deficits that cover physical, biological, social, psychological and cognitive domains. The list of the included deficits in each FI are available in **Supplementary Tables 52-54**. Deficits were either binary (coded as 0 (absent) or 1 (present) or 0.5 to represent a partially present deficit) or were continuous on a scale ranging from 0 to 1. The number of deficits was summed then

divided by the total number of measured deficits to create a proportional FI score for each individual. Resulting FI scores ranged from 0 to 1, with higher scores indicating a higher frailty level. Our FI phenotypes were analyzed using linear regression.

Fried Frailty Phenotype (FP). The FP was only available in LBC1936 and was formed from five physical health traits: weight loss, exhaustion, physical inactivity, walking speed, and grip strength. If an individual did not display any of these 5 traits they were defined as healthy controls, whereas cases included individuals who were classed as being either pre-frail (i.e. the presence of 1-2 of these traits) or frail (i.e. if 3 or more traits were present) (76). We used the FP from waves 1, 3 and 5 in our analyses to assess age-specific differences in physical frailty prediction. This resulted in 483 healthy controls, 514 pre-frail individuals and 94 frail individuals in the Wave 1 sample (used in the main PRS analyses), 268 healthy controls, 327 pre-frail individuals and 102 frail individuals in the Wave 3 sample, and 156 healthy controls, 214 pre-frail individuals and 61 frail individuals in the Wave 5 sample (used in the age-stratified sensitivity PRS analyses). We analyzed the FP phenotype using multinomial logistic regression using non-frail individuals as the reference group.

Frailty-Related Health Outcomes Used for Polygenic Risk Score Prediction

Cognitive Ability and Cognitive Change (N = 1,005). Cognitive ability was measured in LBC1936. This measure was derived from a rich battery of 13 validated cognitive tests administered by psychologists at the initial wave of testing (Wave 1), where participants were ~70 years old. The cognitive tests included Matrix Reasoning, Block Design, Spatial Span, National Adult Reading Test, Wechsler Test of Adult Reading, Verbal Fluency, Verbal Paired Associates, Logical Memory, Digit Span Backwards, Symbol Search, Digit Symbol, Inspection Time and Choice Reaction Time. These were repeated at each subsequent wave (Wave 2: mean age = 72.55, SD = 0.68, *N* = 649 (339 males, 310 females); Wave 3: mean age = 76.30, SD = 0.68, *N* = 649 (339 males, 310 females); Wave 4: mean age = 79.39, SD = 0.62, *N* = 514 (216 males, 298 females) and Wave 5: mean age = 82.06, SD = 0.53, *N* = 402 (196 males, 206 females)). We used the results for all 13 tests to apply latent growth curve (LGC) modelling (i.e., a Factor of Curves model with full information maximum likelihood estimation) to estimate each individual's cognitive ability at Wave 1 (i.e. the intercept estimate; mean age = 69.60) and cognitive change across all waves (i.e. the slope estimate; age 70–82)(77). Individuals were retained in the analysis if they only had baseline data available since the estimates for intercept (cross-sectional) and slope (longitudinal) associations are derived simultaneously from the same model using all available data(78). We then used the *lavpredict* function in the lavaan R package to extract continuous intercept (cognitive ability) and slope (cognitive change) scores for each participant. We used linear regression to assess the association between these outcomes and the frailty PRS's.

Motoric Cognitive Risk (N = 649). Motoric Cognitive Risk (MCR) has been previously derived in LBC1936 (Wave 3) and is a measure that is based on subjective cognitive complaints and objective slow gait with no diagnosed disability or dementia present(79). We defined slow gait speed as walking speed that was one standard deviation below age- and sex-matched means. In LBC1936, this was calculated by digitally timing participants to walk 6 meters. If a participant confirmed that they had problems with memory, in response to the question "Do you currently have any problems with your memory?", this was recorded as a subjective cognitive complaint. Presence of disability or dementia was defined as present if an individual had a Townsend Disability score over 1.5 standard deviation from the mean, a confirmed dementia diagnosis and/or a Mini-Mental State Examination (MMSE) score of < 24/30. To investigate whether any of the frailty PRS's predicted MCR in LBC1936, we used competing risk regression models to examine the risk of developing MCR when death was a competing risk.

Mortality (N = 1,005). We used data from the General Register Office for Scotland to measure deaths in the participants in LBC1936, which we coded as a binary variable (0/1). We included both age in days at death and age at last censor to measure survival via both death and dropout. We conducted survival analysis using Cox proportional hazard regression models to examine the association between time to death and the frailty PRS's. We extracted hazard ratios and standardized beta coefficients from the model to compare effect sizes easily with other outcomes. Of the 1,005 individuals included in the sample, 476 participants had died by Wave 5 in LBC1936, with a mean age of 80 years at death.

Stroke ($N_{LBC1936}$ = 1,005; N_{PISA} = 3,265). We derived the binary stroke measures for LBC1936 and PISA from self-report items where participants were asked whether they had ever had a stroke or a transient

ischemic attack (TIA). We used logistic regression to assess the association between stroke and the frailty PRS outcomes in PISA. We used a competing risk regression model to test for the association between stroke and frailty PRS with dropout as a competing risk in LBC1936 (Wave 1).

Memory Problems (N = 3,265). We utilized the self-report binary variable for memory complaints in PISA as an outcome for memory disturbances, which was derived by asking participants if they "suffer from memory complaints". We used logistic regression to measure the association between memory and the frailty PRS outcomes.

Dementia (N = 1,005). We created a binary variable for self-reported incident dementia in the LBC1936 dataset and analyzed the association between dementia and the frailty PRS outcomes using logistic regression. Of the 1,005 individuals included, 111 individuals received a dementia diagnosis by Wave 5, so were classified as cases in our analysis. The mean age of diagnosis was 80 years.

Cognition (N = 913). We evaluated cognition in the PISA sample using the self-administered online test battery, Creyos (formerly Cambridge Brain Sciences; https://creyos.com). The Creyos battery consists of 12 neurocognitive tasks that assess various cognitive domains, including memory, reasoning, verbal ability, and concentration. The battery takes approximately 30 minutes to complete, with higher scores indicating better performance. Cognitive test scores were standardized then we applied principal component analysis (PCA) with varimax rotation and Kaiser normalization to reduce the dimensionality of the Creyos data to identify three cognitive components that represented visuospatial reasoning, memory and executive function. We used linear regression to assess the association between these three cognitive outcomes and the frailty PRS's from our model.

Supplementary Results

Rationale for Our Interpretation and Naming of the Six Residual Latent Factors

As we outlined in our **Main Results**, we named the six residual latent factors in our model according to the frailty deficits that loaded on to them as a way to interpret what they were most likely to be representing on a biological or clinical level. Below we describe our rationale for the names chosen for each of the latent factors in more detail:

Factor 1 was defined by equal loadings of genetic covariance between not living with a spouse/partner and feeling unable to confide in others. Since this genetic variance was orthogonal to the General Factor of frailty, which included broader psychological deficits within frailty (e.g. major depression, loneliness and feelings of low motivation) and more active aspects of socializing (e.g. low participation in social/leisure activities), we concluded that Factor 1 appears to capture genetic variance linked to "limited social support". By contrast, the General Factor of frailty captured widespread genetic sharing between frailty deficits linked to low mood and social isolation.

Factor 2 was defined by genetic covariance between smoking, arterial stiffness and physical inactivity with similar factor loadings for each deficit, which indicated that they were all having a similar magnitude of effect on the latent factor. We therefore concluded that Factor 2 appears to reflect genetic variance that is associated with "unhealthy lifestyle" because all three deficits are strongly related to behaviors that induce adverse health outcomes(80).

Factor 3 was defined by equal loadings of genetic covariance between number of non-cancer illnesses and high mean arterial pressure. A higher number of non-cancer illnesses also displayed a high factor loading for the General Factor of frailty (which is to be expected since multimorbidity is known to have widespread adverse influences on aging(81)), whereas mean arterial pressure had the lowest factor loading on the General Factor. Therefore, we concluded that Factor 3 likely captures genetic variance associated with cardiovascular-related pathways of "multimorbidity," which is distinct from the general pathways of frailty.

Factor 4 was defined by genetic covariance between high body fat percentage, slow walking pace, basal metabolic rate and shortness of breath walking on flat ground. Compared to the other deficits, basal metabolic rate only had a modest loading on the General Factor of frailty, indicating that it was not being well defined by the general frailty construct. Since the other indicators on Factor 4 were also strongly associated with metabolic syndrome(82-84), we concluded that Factor 4 is most likely representing genetic sharing linked to "metabolic problems".

Factor 5 was defined by genetic covariance between low fluid intelligence score, poor self-reported overall health rating and slow walking pace. The fact that both slow walking pace and poor overall health rating had cross-loadings onto other residual latent factors, whereas low fluid intelligence did not, we concluded that Factor 5 appears to be driven by genetic variance linked to "poorer cognition", since all three deficits have been strongly associated with cognitive function in previous studies(79, 85-87).

Finally, Factor 6 was defined by genetic sharing between poor overall health rating, presence of a long-standing illness, disability or infirmity and diagnosis of an eye disorder/problem. Since this latent factor was strongly negatively correlated with Factor 5, we concluded that Factor 6 appears to capture non-cognitive pathways related to a poorer self-report of health. The high loading of long-standing illness instead of the number of diagnosed illnesses (as seen for Factor 3) indicated that this latent factor may capture genetic variance linked to chronic and long-term "disability". Thereby, we concluded that Factor 6 may be more likely to reflect lifelong pathways of frailty compared to the other latent factors in our model(88).

Genomic Signal of the Latent Frailty Factors

Quantile-Quantile plots of the SNP effects revealed clear genetic signal across all latent frailty factors. Results from linkage disequilibrium score regression (LDSC) further revealed that this reflected meaningful polygenic signal for each latent factor with minimal bias from population confounding. This was evidenced by LD intercept values that were close to 1.0 whereas the mean χ^2 statistics and λ genomic control (λ_{GC}) were inflated (**Supplementary Figure 2 and Table 2**). We also calculated the attenuation ratio for all of the frailty latent factors, which is a more sensitive indicator of confounding for well-powered GWAS traits(89). All the latent factor ratio estimates were <0.20 indicating that our results were not being heavily biased by population stratification(90) (**Table 2**).

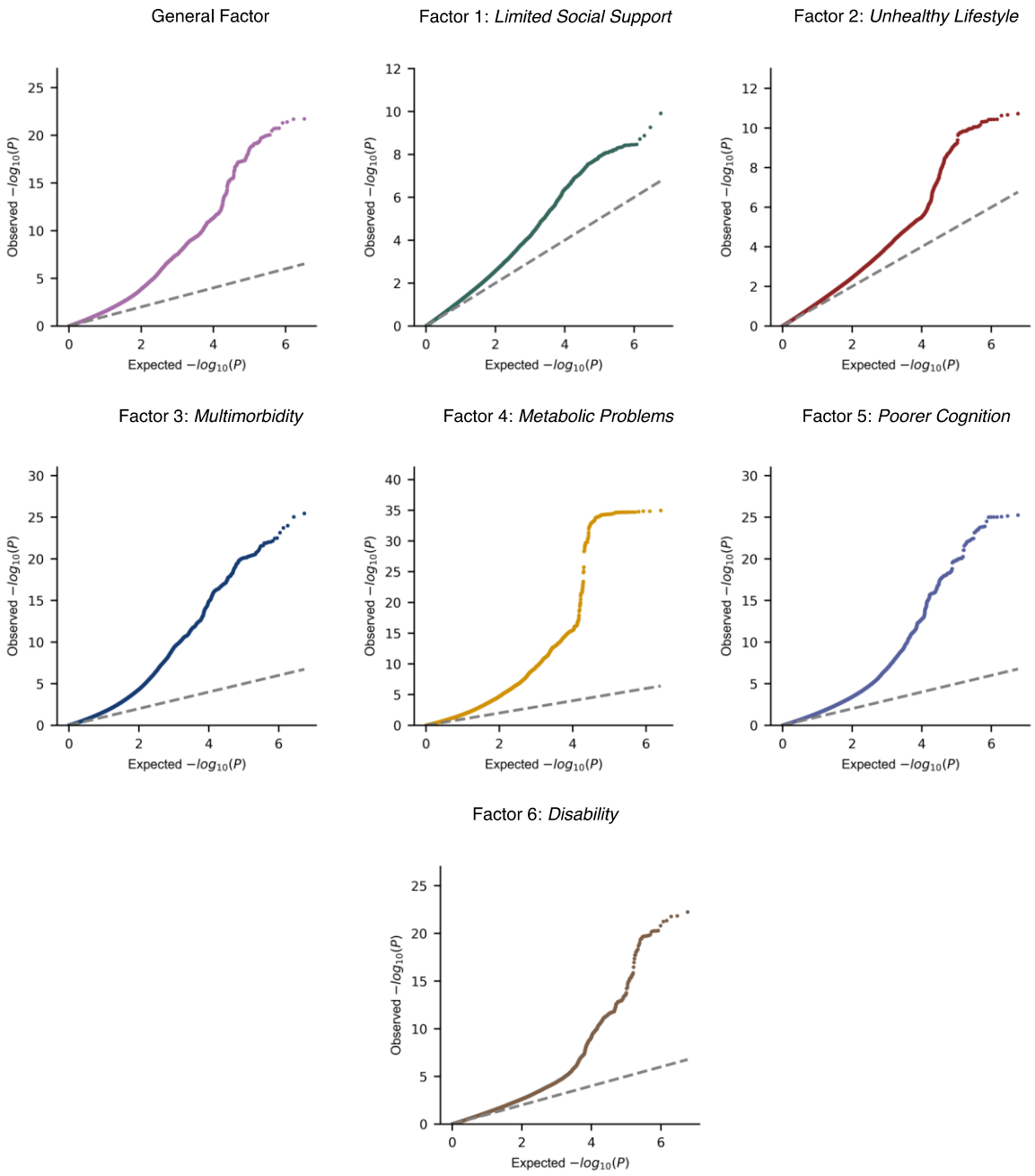

Supplementary Figure 2: Quantile-Quantile (QQ) plots for each latent frailty factor GWAS. The observed SNP -log[10] p-values are plotted on the y-axis and the expected -log[10] p-values are plotted on the x-axis. For all latent frailty factors, there was substantial inflation of the quantile distribution of observed p-values versus the quantile distribution of the expected (i.e. null) p-values.

Table 2: Results from linkage disequilibrium score regression of the GWAS results for each frailty latent factor conducted in Genomic SEM. GC = genomic control; LDSC = linkage disequilibrium score regression; SE = standard error.

Latent Frailty Factor	Mean χ^2	λ GC	LDSC intercept (SE)	Attenuation Ratio
General Factor	1.98	1.78	1.03 (0.02)	0.03 (0.02)
Factor 1 (limited social support)	1.34	1.29	1.05 (0.01)	0.14 (0.03)
Factor 2 (unhealthy lifestyle)	1.28	1.23	0.99 (0.01)	-0.03 (0.03)
Factor 3 (multimorbidity)	2.17	1.84	1.18 (0.02)	0.15 (0.02)
Factor 4 (metabolic problems)	2.40	2.05	1.13 (0.02)	0.09 (0.02)
Factor 5 (poorer cognition)	1.81	1.63	1.10 (0.01)	0.13 (0.02)
Factor 6 (disability)	1.36	1.30	1.07 (0.01)	0.19 (0.03)

Gene Prioritization for the Latent Frailty Factors

We used 5 gene mapping methods (positional, eQTL, chromatin interaction, MAGMA gene-based analysis and summary-data based Mendelian randomization) to identify genes that were potentially driving the shared genetic effects underlying each latent frailty factor. Any gene that was mapped to a latent factor by three or more of these methods was included in our pathway analysis. **Supplementary Figure 3** displays the number of genes mapped by different methods for the General Factor of frailty, and **Supplementary Figure 4** shows how many genes were mapped by the different methodologies for the latent residual factors of frailty (i.e., Factors 1 to 6).

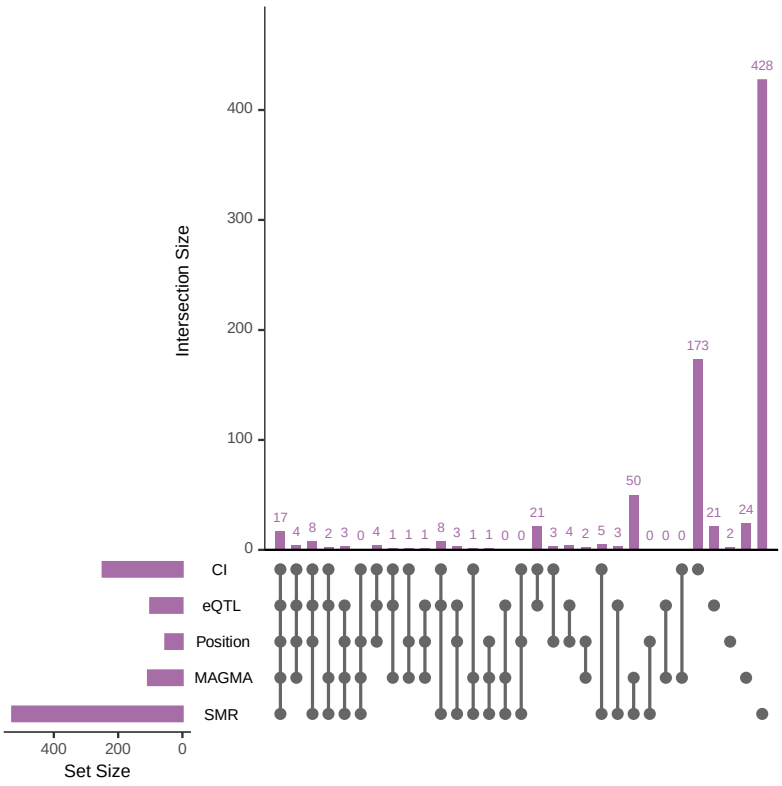

Supplementary Figure 3: An UpSet plot displaying the number of genes mapped to the General Factor of frailty by the 5 different gene mapping methodologies. CI = chromatin interaction; eQTL = expression quantitative trait locus; MAGMA = Multi-marker analysis of genomic annotation gene analysis; SMR = summary data-based Mendelian randomization.

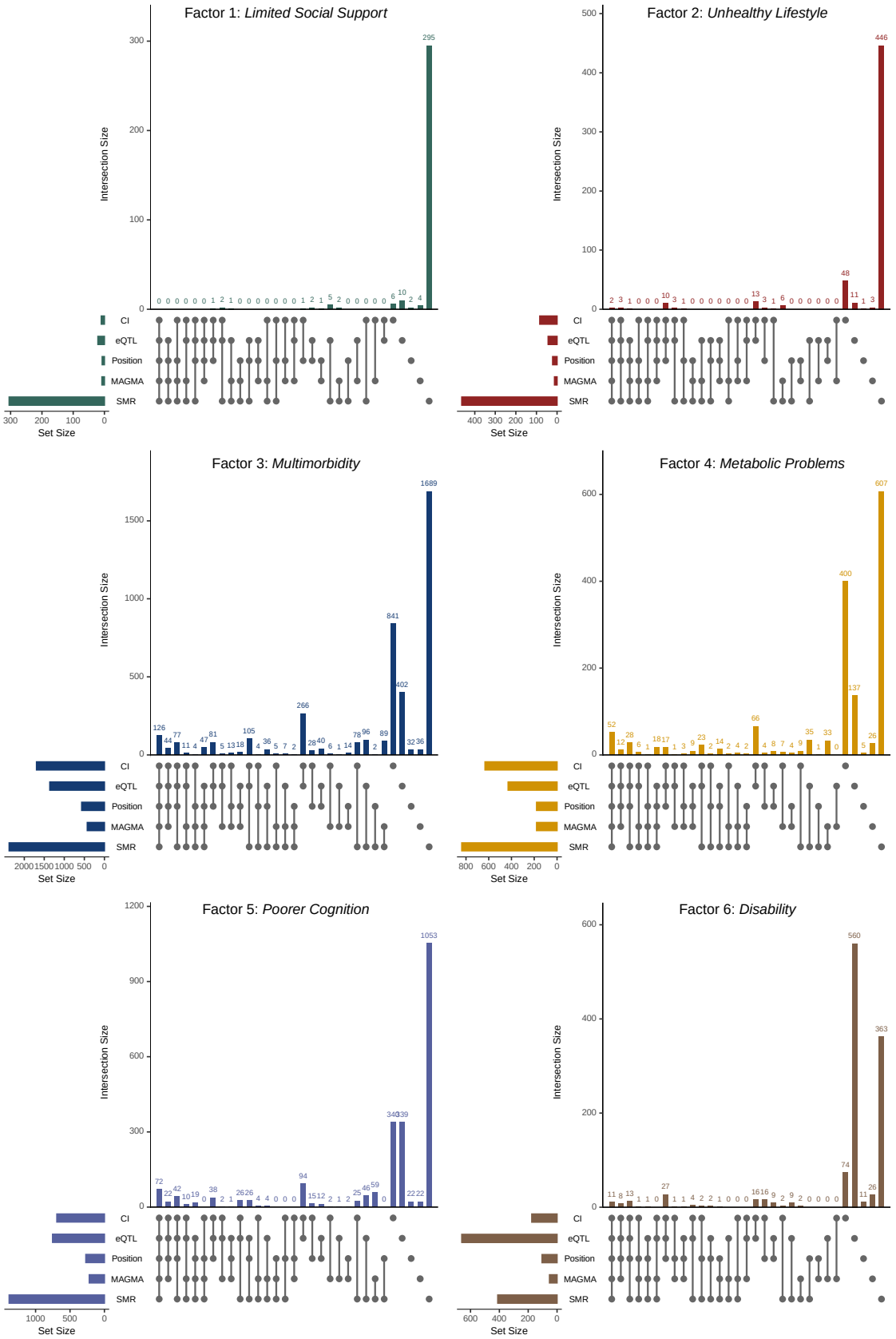

Supplementary Figure 4: UpSet plots displaying the number of genes mapped to the latent residual factors of frailty (i.e., Factors 1-6) by the 5 different gene mapping methodologies. CI = chromatin interaction; eQTL = expression quantitative trait locus; MAGMA = Multi-marker analysis of genomic annotation gene analysis; SMR = summary data-based Mendelian randomization.

Polygenic Risk Scores to Predict Fried Frailty Phenotype Status

As detailed in the main manuscript, we calculated polygenic risk scores (PRS) for each latent frailty factor and used multiple regression to combine these scores into a "Multi-PRS" that captured the genetic variance across all of the latent factors in our model. The PRS for the General Factor of frailty was the strongest predictor of the FP in Waves 1 and 2 of LBC1936, but the Multi-PRS did not significantly predict FP status (**Supplementary Figure 5** and **Supplementary Table 44**). These results suggest that the Multi-PRS is more likely to reflect genetic variance associated with the broader FI phenotype, whereas the General Factor of frailty is more closely aligned to the FP measure of physical frailty.

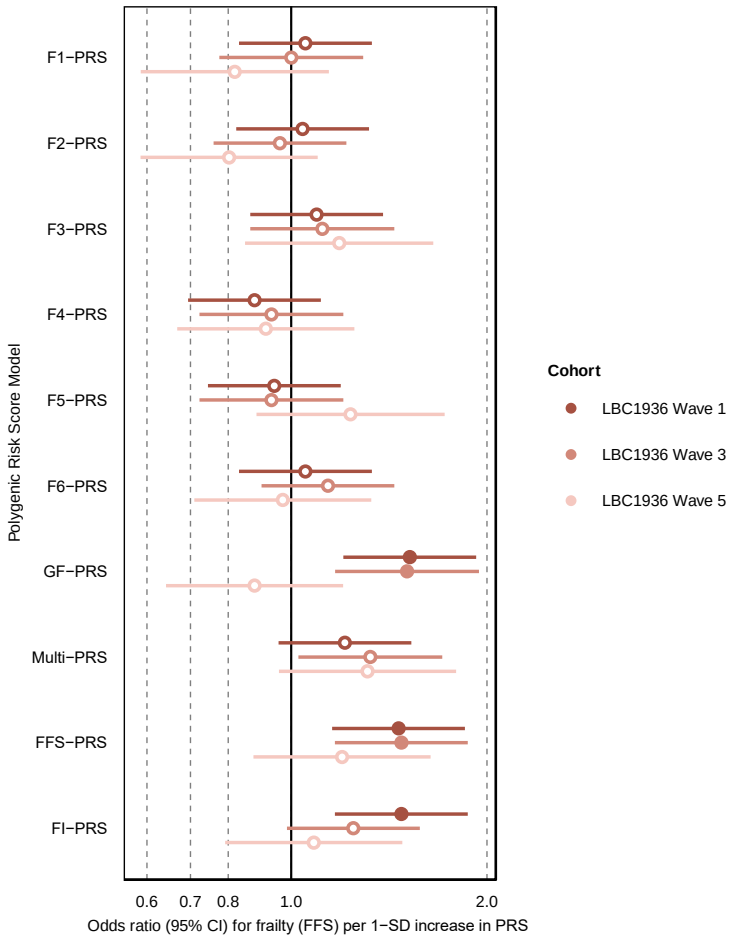

Supplementary Figure 5: Results from the polygenic risk score prediction of the Fried Frailty Phenotype (FP) in the Lothian Birth Cohort 1936 (LBC1936) Waves 1 (*N* = 1005), 3 (*N* = 649) and 5 (*N* = 402). A forest plot comparing the odds ratios for each standard deviation (SD) increase in frailty (measured using the FP) for each of our standardized frailty PRS phenotypes across each wave in LBC1936 calculated using multinomial logistic regression. Error bars represent the 95% confidence intervals. Significant predictions that passed multiple testing correction (i.e. two-sided FDR-corrected *q*-value < 0.05) are depicted as filled in dots, whereas non-significant predictions are depicted as an empty circle. CI = confidence intervals; SD = standard deviation. GF = General Factor; F1-6 = Factors 1-6.

Age-Stratified Polygenic Prediction of Frailty

To assess the prediction of the PRS's for each of our latent frailty factors at different ages, we reran the same multiple regression and elastic net regression analyses as we did in the main analysis in age-stratified samples for ELSA and PISA (i.e. a sub-sample of individuals that were ≥ 65 years old) and data from Waves 3 and 5 of LBC1936. We found a consistent pattern of results with the age-stratified samples as seen in our main analysis, indicating that the latent frailty factors remain valid predictors of frailty statues even in older age groups (**Supplementary Figure 6**).

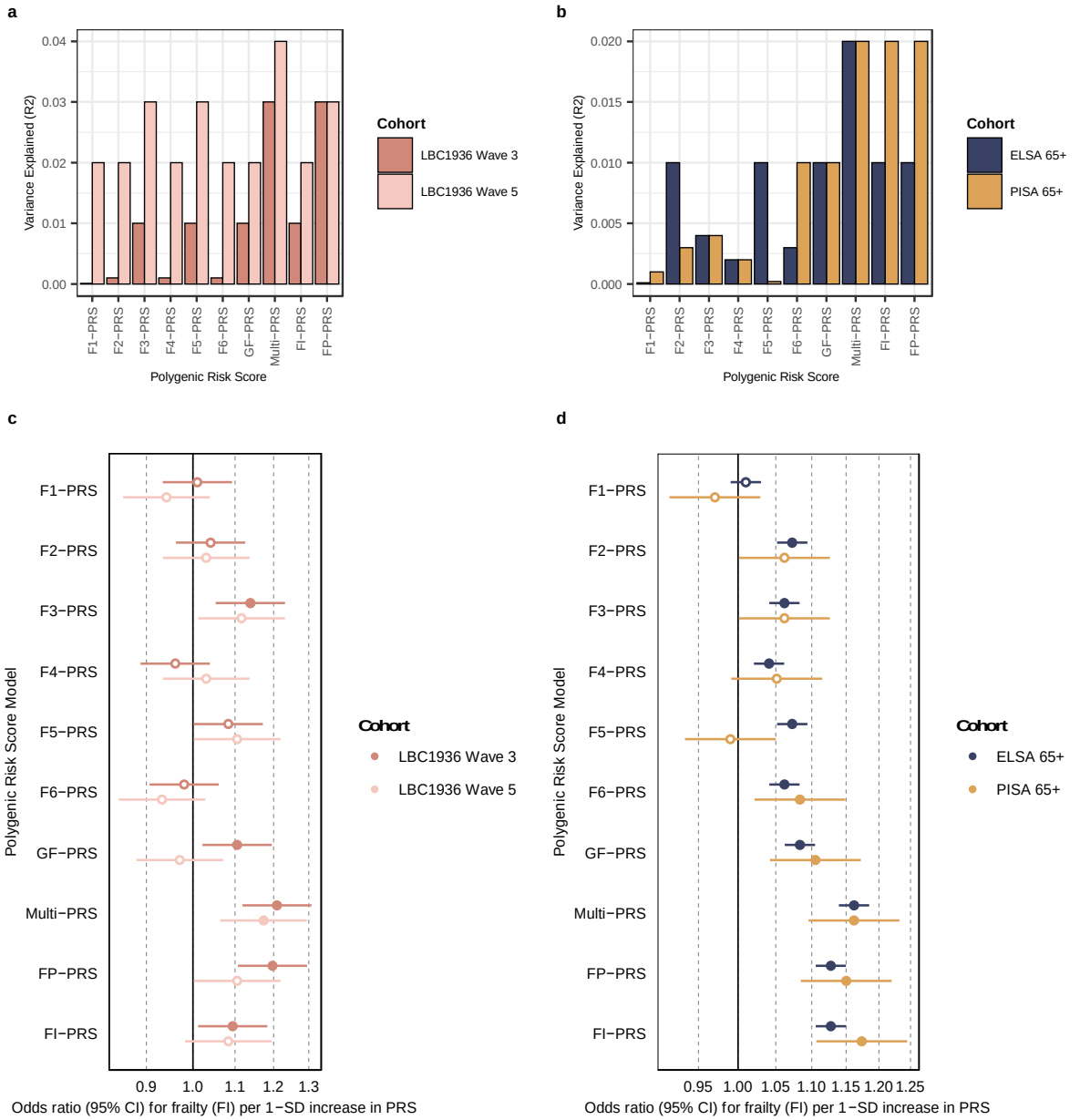

Supplementary Figure 6: Results for age-stratified analyses. *a-b,* Bar plots of the variance explained (R2) by each standardized frailty polygenic risk score (PRS) for predicting frailty status (measured by the Frailty Index) in the age-stratified samples from the external cohorts. ***c-d,*** Forest plots of the association between Frailty Index status and our standardized frailty PRS phenotypes in the age-stratified samples from external cohorts. Data are displayed as odds ratios for each standard deviation (SD) increase in frailty as the point estimate with their 95% confidence intervals as the error bars. Significant predictions that passed multiple testing correction (i.e. two-sided FDR-corrected *q*-value < 0.05) are depicted as filled in dots. Across all panels, the samples for LBC1936 represents Wave 3 (*N* = 649) and Wave 5 (*N* = 402) of the data, whereas for ELSA and PISA the samples only included individuals aged ≥ 65 years (*N*= 2341 and *N* = 991, respectively). LBC1936 = Lothian Birth Cohort 1936; PISA = Prospective Imaging Study of Aging; ELSA = English Longitudinal Study of Aging; F1-F6 = Factors 1-6; GF = General Factor; FI = Frailty Index; FP = Fried Frailty Phenotype; PRS = polygenic risk score.

We then used elastic net regression to rank the predictive contributions of the PRS for each of the seven latent frailty factors from our model in the subsamples of individuals aged ≥ 65 years from PISA and ELSA. We included sex, age and ancestral principal components as covariates. The PRS for the General Factor of frailty remained the best predictor of FI status in both cohorts and the unique predictive contributions from the PRS's for the six latent residual factors of frailty (i.e., Factors 1-6) remained relatively stable in the older age groups (**Supplementary Figure 7a-b**).

Finally, we used elastic net regression to compare the predictive performance of our Multi-PRS against the aggregate FI-PRS and FP-PRS measures in a model that also included age, sex and 10 ancestral principal components as covariates, which we tested in the ELSA and PISA subsamples of individuals aged ≥ 65 years (**Supplementary Figure 7c-d**). We found that the Multi-PRS provided additional unique frailty status prediction in both cohorts, and outperformed both previously used aggregate frailty measures in the ELSA sample. Age became more predictive in the older age group for both cohorts, which is to be expected because age is strongly associated with frailty risk. We also identified a large predictive effect of sex on frailty status in both ELSA and PISA.

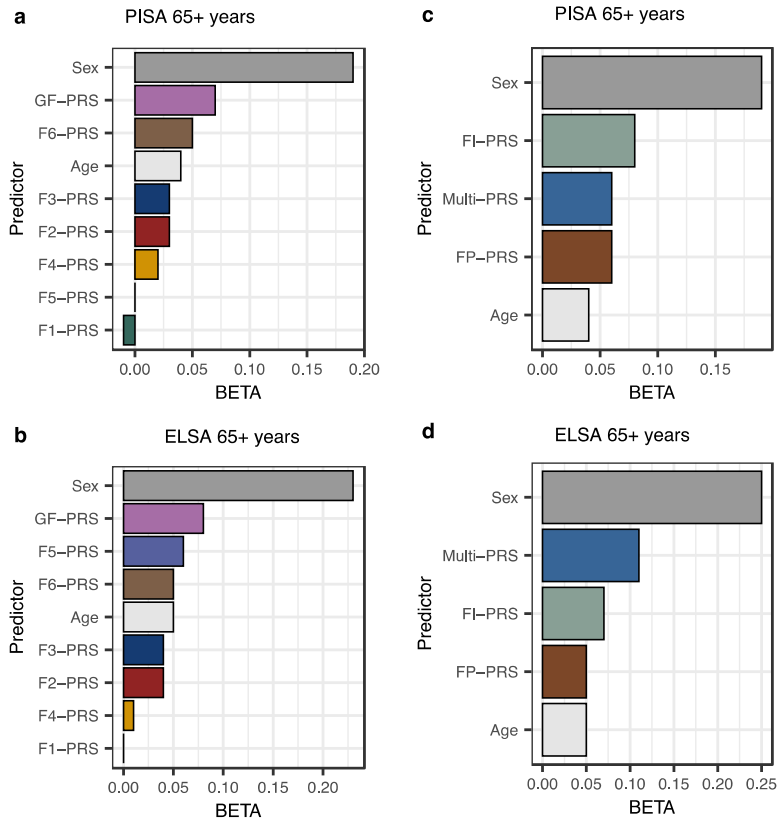

Supplementary Figure 7: Results for the age-stratified elastic net regression results in ELSA (*N* = 2341) and PISA (*N* = 991). *a-b,* Bar plots of the beta coefficients (x-axis) from the age-stratified elastic net regression analysis, which rank the contributions of the seven latent frailty factors in predicting Frailty Index status in the older ELSA and PISA subgroups (i.e. individuals aged ≥ 65 years) on the y-axis. Each model included all seven latent factor PRS's as well as age, sex and ancestral principal components as covariates. ***c-d,*** Bar plots of the beta coefficients (x-axis) from the age-stratified elastic net regression analyses that ranked the performance of our Multi-PRS (i.e. combined latent frailty factor score) when modelled with the aggregate Frailty Index PRS (FI-PRS), the aggregate Fried Frailty Phenotype PRS (FP-PRS), age, sex and ancestral principal components as covariates (y-axis). PRS = polygenic risk score; GF = General Factor; F1-6 = Factors 1-6; PISA = Prospective Imaging Study of Aging; ELSA = English Longitudinal Study of Aging.

Simulation Results of New Method to Calculate Q_{SNP} Heterogeneity Index

As we outlined in the main text, we developed a more computationally tractable method to calculate the factor-specific Q_{SNP} heterogeneity index for each measured SNP in a multivariate GWAS conducted within Genomic SEM. To validate this new closed-form method against the model comparison method previously introduced by Grotzinger et al.(3), we simulated 3 different factor models, including a 2-factor model with three indicators on each factor (2 degrees of freedom [df]), a 2-factor model with four indicators on each factor (3 df) and a 2-factor model with six indicators on each factor (5 df). **Table 3** and **Supplementary Figure 8** provide evidence that there was not a significant difference in the mean Q_{SNP} estimates between the closed-form estimation versus the model comparison method and that our closed-form method remained χ^2-distributed at a comparable level to the model comparison method. **Table 4** further demonstrates that the closed-form method produced a slightly lower type 1 error rate compared to the model comparison method.

Table 3: Comparisons of the closed-form and model comparison Q_{SNP} estimation methods from our simulation tests. SD = standard deviation; df = degrees of freedom.

Simulation Model	Closed-Form Method		Model Comparison Method		Mean difference between closed-form and model comparison method
	Mean Q_{SNP} estimate	*SD of Q_{SNP} estimate*	*Mean Q_{SNP} estimate*	*SD of Q_{SNP} estimate*	
2 df model	2.004	1.939	2.049	1.984	-0.044
3 df model	3.050	2.503	3.099	2.543	-0.049
5 df model	4.951	3.099	5.009	3.146	-0.058

Table 4: Comparison of type-1 error rates between the closed-form and model comparison Q_{SNP} estimation methods. Df = degrees of freedom.

Simulation Model	Closed-Form Method			Model Comparison Method		
	Number of type 1 errors	*Number of non-type-1 errors*	*Ratio*	*Number of type 1 errors*	*Number of non-type-1 errors*	*Ratio*
2 df model	46	954	0.046	49	951	0.049
3 df model	49	951	0.049	52	948	0.052
5 df model	41	959	0.041	47	953	0.047

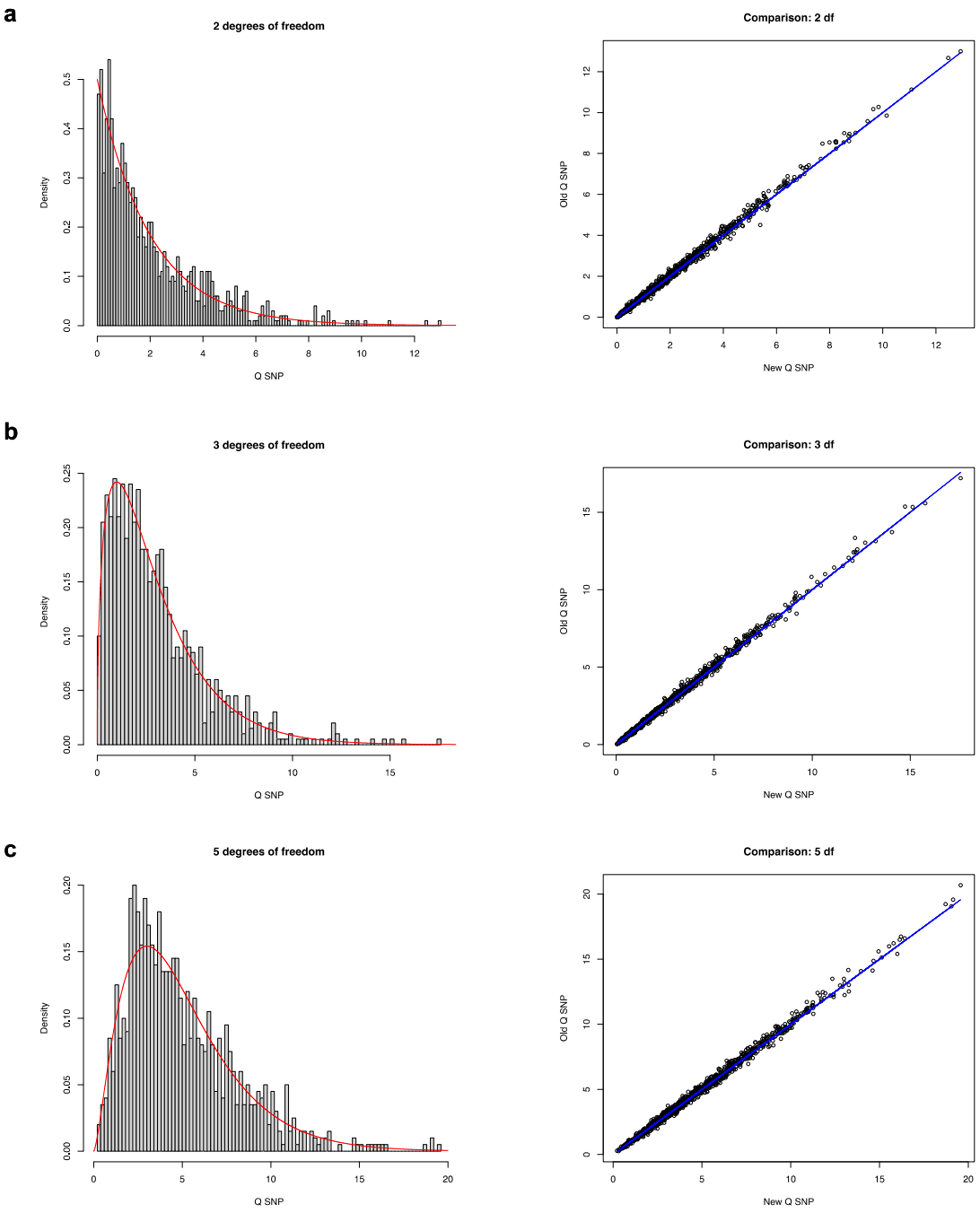

Supplementary Figure 8: Distributions of the Q_{SNP} χ^2 statistics of our simulated models. Each model was based on simulated data each with 50,000 observations for 1000 SNPs as the sample size. Left-hand plots depict histograms of the distributions for the simulated Q_{SNP} χ^2 statistics on the x-axis generated using the new closed-form estimation method within the *GenomicSEM* R package and the right-hand plots present scatter plots of the Q_{SNP} χ^2 statistics generated from the old estimation method on the y-axis and the new estimation method on the x-axis. **a,** Shows the results for the 2df model (2 factors with 3 indicators) **b,** shows the 3df model results (2 factors with 4 indicators) and, **c,** shows the 5df model results (2 factors with 6 indicators).

References

1. Bulik-Sullivan B, Finucane HK, Anttila V, Gusev A, Day FR, Loh P-R, et al. An atlas of genetic correlations across human diseases and traits. Nature Genetics. 2015;47(11):1236-41.
2. Bulik-Sullivan B, Loh P-R, Finucane HK, Ripke S, Yang J, Patterson N, et al. LD Score regression distinguishes confounding from polygenicity in genome-wide association studies. Nature Genetics. 2015;47(3):291-5.
3. Grotzinger AD, Rhemtulla M, de Vlaming R, Ritchie SJ, Mallard TT, Hill WD, et al. Genomic structural equation modelling provides insights into the multivariate genetic architecture of complex traits. Nat Hum Behav. 2019;3(5):513-25.
4. Zheng J, Erzurumluoglu AM, Elsworth BL, Kemp JP, Howe L, Haycock PC, et al. LD Hub: a centralized database and web interface to perform LD score regression that maximizes the potential of summary level GWAS data for SNP heritability and genetic correlation analysis. Bioinformatics. 2016;33(2):272-9.
5. Grotzinger AD, Mallard TT, Akingbuwa WA, Ip HF, Adams MJ, Lewis CM, et al. Genetic architecture of 11 major psychiatric disorders at biobehavioral, functional genomic and molecular genetic levels of analysis. Nature Genetics. 2022;54(5):548-59.
6. Chawla K, Kunonga TP, Stow D, Barker R, Craig D, Hanratty B. Prevalence of loneliness amongst older people in high-income countries: A systematic review and meta-analysis. PLOS ONE. 2021;16(7):e0255088.
7. Livingston G, Huntley J, Sommerlad A, Ames D, Ballard C, Banerjee S, et al. Dementia prevention, intervention, and care: 2020 report of the Lancet Commission. The Lancet. 2020;396(10248):413-46.
8. Lisan Q, Goldberg M, Lahlou G, Ozguler A, Lemonnier S, Jouven X, et al. Prevalence of Hearing Loss and Hearing Aid Use Among Adults in France in the CONSTANCES Study. JAMA Network Open. 2022;5(6):e2217633-e.
9. Evans JR, Fletcher AE, Wormald RPL, Ng ES-W, Stirling S, Smeeth L, et al. Prevalence of visual impairment in people aged 75 years and older in Britain: results from the MRC trial of assessment and management of older people in the community. British Journal of Ophthalmology. 2002;86(7):795.
10. Kerkhof GA. Epidemiology of sleep and sleep disorders in The Netherlands. Sleep Medicine. 2017;30:229-39.
11. Pratt J, De Vito G, Narici M, Segurado R, Dolan J, Conroy J, et al. Grip strength performance from 9431 participants of the GenoFit study: normative data and associated factors. GeroScience. 2021;43(5):2533-46.
12. Salari N, Darvishi N, Ahmadipanah M, Shohaimi S, Mohammadi M. Global prevalence of falls in the older adults: a comprehensive systematic review and meta-analysis. Journal of Orthopaedic Surgery and Research. 2022;17(1):334.
13. Verschoor CP, Cakmak S, Lukina AO, Dales RE. Activity-related dyspnea in older adults participating in the Canadian Longitudinal Study on Aging. Journal of General Internal Medicine. 2022;37(13):3302-9.
14. Kotwal AA, Cenzer IS, Waite LJ, Covinsky KE, Perissinotto CM, Boscardin WJ, et al. The epidemiology of social isolation and loneliness among older adults during the last years of life. Journal of the American Geriatrics Society. 2021;69(11):3081-91.
15. Grotzinger AD, Fuente Jdl, Privé F, Nivard MG, Tucker-Drob EM. Pervasive Downward Bias in Estimates of Liability-Scale Heritability in Genome-wide Association Study Meta-analysis: A Simple Solution. Biological Psychiatry. 2023;93(1):29-36.
16. Murphy AE, Schilder BM, Skene NG. MungeSumstats: a Bioconductor package for the standardization and quality control of many GWAS summary statistics. Bioinformatics. 2021;37(23):4593-6.
17. Watanabe K, Taskesen E, van Bochoven A, Posthuma D. Functional mapping and annotation of genetic associations with FUMA. Nat Commun. 2017;8(1):1826.
18. Westra H-J, Peters MJ, Esko T, Yaghootkar H, Schurmann C, Kettunen J, et al. Systematic identification of trans eQTLs as putative drivers of known disease associations. Nature Genetics. 2013;45(10):1238-43.
19. Zhernakova DV, Deelen P, Vermaat M, van Iterson M, van Galen M, Arindrarto W, et al. Identification of context-dependent expression quantitative trait loci in whole blood. Nature Genetics. 2017;49(1):139-45.

20. Ramasamy A, Trabzuni D, Guelfi S, Varghese V, Smith C, Walker R, et al. Genetic variability in the regulation of gene expression in ten regions of the human brain. Nature Neuroscience. 2014;17(10):1418-28.
21. Grundberg E, Small KS, Hedman ÅK, Nica AC, Buil A, Keildson S, et al. Mapping cis- and trans-regulatory effects across multiple tissues in twins. Nature Genetics. 2012;44(10):1084-9.
22. Ng B, White CC, Klein H-U, Sieberts SK, McCabe C, Patrick E, et al. An xQTL map integrates the genetic architecture of the human brain's transcriptome and epigenome. Nature Neuroscience. 2017;20(10):1418-26.
23. Fromer M, Roussos P, Sieberts SK, Johnson JS, Kavanagh DH, Perumal TM, et al. Gene expression elucidates functional impact of polygenic risk for schizophrenia. Nature Neuroscience. 2016;19(11):1442-53.
24. Võsa U, Claringbould A, Westra H-J, Bonder MJ, Deelen P, Zeng B, et al. Large-scale cis- and trans-eQTL analyses identify thousands of genetic loci and polygenic scores that regulate blood gene expression. Nature Genetics. 2021;53(9):1300-10.
25. Wang D, Liu S, Warrell J, Won H, Shi X, Navarro FCP, et al. Comprehensive functional genomic resource and integrative model for the human brain. Science. 2018;362(6420):eaat8464.
26. Schmiedel BJ, Singh D, Madrigal A, Valdovino-Gonzalez AG, White BM, Zapardiel-Gonzalo J, et al. Impact of Genetic Polymorphisms on Human Immune Cell Gene Expression. Cell. 2018;175(6):1701-15.e16.
27. van der Wijst MGP, Brugge H, de Vries DH, Deelen P, Swertz MA, Franke L, et al. Single-cell RNA sequencing identifies celltype-specific cis-eQTLs and co-expression QTLs. Nature Genetics. 2018;50(4):493-7.
28. Alasoo K, Rodrigues J, Mukhopadhyay S, Knights AJ, Mann AL, Kundu K, et al. Shared genetic effects on chromatin and gene expression indicate a role for enhancer priming in immune response. Nature Genetics. 2018;50(3):424-31.
29. Chen L, Ge B, Casale FP, Vasquez L, Kwan T, Garrido-Martín D, et al. Genetic Drivers of Epigenetic and Transcriptional Variation in Human Immune Cells. Cell. 2016;167(5):1398-414.e24.
30. Jaffe AE, Straub RE, Shin JH, Tao R, Gao Y, Collado-Torres L, et al. Developmental and genetic regulation of the human cortex transcriptome illuminate schizophrenia pathogenesis. Nature Neuroscience. 2018;21(8):1117-25.
31. Momozawa Y, Dmitrieva J, Théâtre E, Deffontaine V, Rahmouni S, Charloteaux B, et al. IBD risk loci are enriched in multigenic regulatory modules encompassing putative causative genes. Nature Communications. 2018;9(1):2427.
32. Fairfax BP, Humburg P, Makino S, Naranbhai V, Wong D, Lau E, et al. Innate Immune Activity Conditions the Effect of Regulatory Variants upon Monocyte Gene Expression. Science. 2014;343(6175):1246949.
33. Fairfax BP, Makino S, Radhakrishnan J, Plant K, Leslie S, Dilthey A, et al. Genetics of gene expression in primary immune cells identifies cell type–specific master regulators and roles of HLA alleles. Nature Genetics. 2012;44(5):502-10.
34. Gutierrez-Arcelus M, Lappalainen T, Montgomery SB, Buil A, Ongen H, Yurovsky A, et al. Passive and active DNA methylation and the interplay with genetic variation in gene regulation. eLife. 2013;2:e00523.
35. Lappalainen T, Sammeth M, Friedländer MR, ‘t Hoen PAC, Monlong J, Rivas MA, et al. Transcriptome and genome sequencing uncovers functional variation in humans. Nature. 2013;501(7468):506-11.
36. Kilpinen H, Goncalves A, Leha A, Afzal V, Alasoo K, Ashford S, et al. Common genetic variation drives molecular heterogeneity in human iPSCs. Nature. 2017;546(7658):370-5.
37. Kasela S, Kisand K, Tserel L, Kaleviste E, Remm A, Fischer K, et al. Pathogenic implications for autoimmune mechanisms derived by comparative eQTL analysis of CD4+ versus CD8+ T cells. PLOS Genetics. 2017;13(3):e1006643.
38. Lepik K, Annilo T, Kukuškina V, e QC, Kisand K, Kutalik Z, et al. C-reactive protein upregulates the whole blood expression of CD59 - an integrative analysis. PLOS Computational Biology. 2017;13(9):e1005766.
39. Naranbhai V, Fairfax BP, Makino S, Humburg P, Wong D, Ng E, et al. Genomic modulators of gene expression in human neutrophils. Nature Communications. 2015;6(1):7545.
40. Nédélec Y, Sanz J, Baharian G, Szpiech ZA, Pacis A, Dumaine A, et al. Genetic Ancestry and Natural Selection Drive Population Differences in Immune Responses to Pathogens. Cell. 2016;167(3):657-69.e21.

41. Quach H, Rotival M, Pothlichet J, Loh Y-HE, Dannemann M, Zidane N, et al. Genetic Adaptation and Neandertal Admixture Shaped the Immune System of Human Populations. Cell. 2016;167(3):643-56.e17.
42. Schwartzentruber J, Foskolou S, Kilpinen H, Rodrigues J, Alasoo K, Knights AJ, et al. Molecular and functional variation in iPSC-derived sensory neurons. Nature Genetics. 2018;50(1):54-61.
43. Buil A, Brown AA, Lappalainen T, Viñuela A, Davies MN, Zheng H-F, et al. Gene-gene and gene-environment interactions detected by transcriptome sequence analysis in twins. Nature Genetics. 2015;47(1):88-91.
44. van de Bunt M, Manning Fox JE, Dai X, Barrett A, Grey C, Li L, et al. Transcript Expression Data from Human Islets Links Regulatory Signals from Genome-Wide Association Studies for Type 2 Diabetes and Glycemic Traits to Their Downstream Effectors. PLOS Genetics. 2015;11(12):e1005694.
45. Aguet F, Anand S, Ardlie KG, Gabriel S, Getz GA, Graubert A, et al. The GTEx Consortium atlas of genetic regulatory effects across human tissues. Science. 2020;369(6509):1318-30.
46. Ratnapriya R, Sosina OA, Starostik MR, Kwicklis M, Kapphahn RJ, Fritsche LG, et al. Retinal transcriptome and eQTL analyses identify genes associated with age-related macular degeneration. Nature Genetics. 2019;51(4):606-10.
47. Viñuela A, Varshney A, van de Bunt M, Prasad RB, Asplund O, Bennett A, et al. Genetic variant effects on gene expression in human pancreatic islets and their implications for T2D. Nature Communications. 2020;11(1):4912.
48. Alonso L, Piron A, Morán I, Guindo-Martínez M, Bonàs-Guarch S, Atla G, et al. TIGER: The gene expression regulatory variation landscape of human pancreatic islets. Cell Reports. 2021;37(2):109807.
49. Schmitt Anthony D, Hu M, Jung I, Xu Z, Qiu Y, Tan Catherine L, et al. A Compendium of Chromatin Contact Maps Reveals Spatially Active Regions in the Human Genome. Cell Reports. 2016;17(8):2042-59.
50. Andersson R, Gebhard C, Miguel-Escalada I, Hoof I, Bornholdt J, Boyd M, et al. An atlas of active enhancers across human cell types and tissues. Nature. 2014;507(7493):455-61.
51. Giusti-Rodríguez P, Lu L, Yang Y, Crowley CA, Liu X, Juric I, et al. Using three-dimensional regulatory chromatin interactions from adult and fetal cortex to interpret genetic results for psychiatric disorders and cognitive traits. bioRxiv. 2019:406330.
52. Kundaje A, Meuleman W, Ernst J, Bilenky M, Yen A, Heravi-Moussavi A, et al. Integrative analysis of 111 reference human epigenomes. Nature. 2015;518(7539):317-30.
53. Haycock PC, Burgess S, Wade KH, Bowden J, Relton C, Davey Smith G. Best (but oft-forgotten) practices: the design, analysis, and interpretation of Mendelian randomization studies. Am J Clin Nutr. 2016;103(4):965-78.
54. Wu Y, Zeng J, Zhang F, Zhu Z, Qi T, Zheng Z, et al. Integrative analysis of omics summary data reveals putative mechanisms underlying complex traits. Nature Communications. 2018;9(1):918.
55. Zhu Z, Zhang F, Hu H, Bakshi A, Robinson MR, Powell JE, et al. Integration of summary data from GWAS and eQTL studies predicts complex trait gene targets. Nature Genetics. 2016;48(5):481-7.
56. Qi T, Wu Y, Fang H, Zhang F, Liu S, Zeng J, et al. Genetic control of RNA splicing and its distinct role in complex trait variation. Nature Genetics. 2022;54(9):1355-63.
57. Lloyd-Jones LR, Holloway A, McRae A, Yang J, Small K, Zhao J, et al. The Genetic Architecture of Gene Expression in Peripheral Blood. The American Journal of Human Genetics. 2017;100(2):228-37.
58. Gandal MJ, Zhang P, Hadjimichael E, Walker RL, Chen C, Liu S, et al. Transcriptome-wide isoform-level dysregulation in ASD, schizophrenia, and bipolar disorder. Science. 2018;362(6420):eaat8127.
59. Qi T, Wu Y, Zeng J, Zhang F, Xue A, Jiang L, et al. Identifying gene targets for brain-related traits using transcriptomic and methylomic data from blood. Nature Communications. 2018;9(1):2282.
60. McRae AF, Marioni RE, Shah S, Yang J, Powell JE, Harris SE, et al. Identification of 55,000 Replicated DNA Methylation QTL. Scientific Reports. 2018;8(1):17605.
61. Zhou Y, Zhou B, Pache L, Chang M, Khodabakhshi AH, Tanaseichuk O, et al. Metascape provides a biologist-oriented resource for the analysis of systems-level datasets. Nat Commun. 2019;10(1):1523.
62. Consortium TGO, Aleksander SA, Balhoff J, Carbon S, Cherry JM, Drabkin HJ, et al. The Gene Ontology knowledgebase in 2023. Genetics. 2023;224(1).
63. Liberzon A, Birger C, Thorvaldsdóttir H, Ghandi M, Mesirov JP, Tamayo P. The Molecular Signatures Database (MSigDB) hallmark gene set collection. Cell systems. 2015;1(6):417-25.
64. Jassal B, Matthews L, Viteri G, Gong C, Lorente P, Fabregat A, et al. The reactome pathway knowledgebase. Nucleic Acids Research. 2019;48(D1):D498-D503.

65. Kanehisa M, Furumichi M, Sato Y, Kawashima M, Ishiguro-Watanabe M. KEGG for taxonomy-based analysis of pathways and genomes. Nucleic Acids Research. 2022;51(D1):D587-D92.
66. Agrawal A, Balcı H, Hanspers K, Coort SL, Martens M, Slenter DN, et al. WikiPathways 2024: next generation pathway database. Nucleic Acids Research. 2023;52(D1):D679-D89.
67. Piñero J, Bravo À, Queralt-Rosinach N, Gutiérrez-Sacristán A, Deu-Pons J, Centeno E, et al. DisGeNET: a comprehensive platform integrating information on human disease-associated genes and variants. Nucleic Acids Research. 2016;45(D1):D833-D9.
68. Taylor AM, Pattie A, Deary IJ. Cohort Profile Update: The Lothian Birth Cohorts of 1921 and 1936. International Journal of Epidemiology. 2018;47(4):1042-r.
69. Houlihan LM, Davies G, Tenesa A, Harris SE, Luciano M, Gow AJ, et al. Common Variants of Large Effect in F12, KNG1, and HRG Are Associated with Activated Partial Thromboplastin Time. The American Journal of Human Genetics. 2010;86(4):626-31.
70. Steptoe A, Breeze E, Banks J, Nazroo J. Cohort Profile: The English Longitudinal Study of Ageing. International Journal of Epidemiology. 2012;42(6):1640-8.
71. Flint JP, Welstead M, Cox SR, Russ TC, Marshall A, Luciano M. Validation of a polygenic risk score for frailty in the Lothian Birth Cohort 1936 and English longitudinal study of ageing. Scientific Reports. 2024;14(1):12586.
72. Lupton MK, Robinson GA, Adam RJ, Rose S, Byrne GJ, Salvado O, et al. A prospective cohort study of prodromal Alzheimer's disease: Prospective Imaging Study of Ageing: Genes, Brain and Behaviour (PISA). NeuroImage: Clinical. 2021;29:102527.
73. Cuellar-Partida G, Springelkamp H, Lucas SEM, Yazar S, Hewitt AW, Iglesias AI, et al. WNT10A exonic variant increases the risk of keratoconus by decreasing corneal thickness. Human Molecular Genetics. 2015;24(17):5060-8.
74. Medland SE, Nyholt DR, Painter JN, McEvoy BP, McRae AF, Zhu G, et al. Common Variants in the Trichohyalin Gene Are Associated with Straight Hair in Europeans. The American Journal of Human Genetics. 2009;85(5):750-5.
75. McCarthy S, Das S, Kretzschmar W, Delaneau O, Wood AR, Teumer A, et al. A reference panel of 64,976 haplotypes for genotype imputation. Nature Genetics. 2016;48(10):1279-83.
76. Welstead M, Muniz-Terrera G, Russ TC, Corley J, Taylor AM, Gale CR, et al. Inflammation as a risk factor for the development of frailty in the Lothian Birth Cohort 1936. Exp Gerontol. 2020;139:111055.
77. Corley J, Conte F, Harris SE, Taylor AM, Redmond P, Russ TC, et al. Predictors of longitudinal cognitive ageing from age 70 to 82 including APOE e4 status, early-life and lifestyle factors: the Lothian Birth Cohort 1936. Molecular Psychiatry. 2023;28(3):1256-71.
78. Altschul DM, Deary IJ. Playing Analog Games Is Associated With Reduced Declines in Cognitive Function: A 68-Year Longitudinal Cohort Study. The Journals of Gerontology: Series B. 2019;75(3):474-82.
79. Mullin DS, Gadd D, Russ TC, Luciano M, Muniz-Terrera G. Motoric cognitive risk syndrome trajectories and incident dementia over 10 years. Cerebral Circulation - Cognition and Behavior. 2023;5:100178.
80. Vasan RS, Pan S, Xanthakis V, Beiser A, Larson MG, Seshadri S, et al. Arterial Stiffness and Long-Term Risk of Health Outcomes: The Framingham Heart Study. Hypertension. 2022;79(5):1045-56.
81. Fabbri E, Zoli M, Gonzalez-Freire M, Salive ME, Studenski SA, Ferrucci L. Aging and Multimorbidity: New Tasks, Priorities, and Frontiers for Integrated Gerontological and Clinical Research. J Am Med Dir Assoc. 2015;16(8):640-7.
82. Vásquez-Alvarez S, Bustamante-Villagomez SK, Vazquez-Marroquin G, Porchia LM, Pérez-Fuentes R, Torres-Rasgado E, et al. Metabolic Age, an Index Based on Basal Metabolic Rate, Can Predict Individuals That are High Risk of Developing Metabolic Syndrome. High Blood Pressure & Cardiovascular Prevention. 2021;28(3):263-70.
83. Fahed G, Aoun L, Bou Zerdan M, Allam S, Bou Zerdan M, Bouferraa Y, et al. Metabolic Syndrome: Updates on Pathophysiology and Management in 2021. Int J Mol Sci. 2022;23(2).
84. Thorsen T, Oliveira N, Graybeal A, Stavres J. Exploring gait velocity as a predictor of cardiometabolic disease risk in young adults. Frontiers in Sports and Active Living. 2024;6.
85. Parfenov VA, Zakharov VV, Kabaeva AR, Vakhnina NV. Subjective cognitive decline as a predictor of future cognitive decline: a systematic review. Dement Neuropsychol. 2020;14(3):248-57.
86. Gao P-Y, Ma L-Z, Wang X-J, Wu B-S, Huang Y-M, Wang Z-B, et al. Physical frailty, genetic predisposition, and incident dementia: a large prospective cohort study. Translational Psychiatry. 2024;14(1):212.

87. Samu D, Campbell KL, Tsvetanov KA, Shafto MA, Brayne C, Bullmore ET, et al. Preserved cognitive functions with age are determined by domain-dependent shifts in network responsivity. Nature Communications. 2017;8(1):14743.
88. Evenhuis H, Schoufour J, Echteld M. Frailty and intellectual disability: A different operationalization? Developmental Disabilities Research Reviews. 2013;18(1):17-21.
89. Loh P-R, Kichaev G, Gazal S, Schoech AP, Price AL. Mixed-model association for biobank-scale datasets. Nature Genetics. 2018;50(7):906-8.
90. Wang Y, Namba S, Lopera E, Kerminen S, Tsuo K, Läll K, et al. Global Biobank analyses provide lessons for developing polygenic risk scores across diverse cohorts. Cell Genomics. 2023;3(1).